The Integer Quantum Hall Effect

Aly Abouzaid, Jun Dai, Simon Feiler, Philipp Kessler, and Chris Waddell

The integer quantum Hall effect concerns the transport properties of a 2-dimensional electron system in the presence of a magnetic field. We analyze the theoretical underpinnings of this effect, emphasizing in particular the role of disorder and topological considerations. We proceed to review the classic experiment of von Klitzing et al. [1], which provided the earliest experimental confirmation of exact quantization of Hall conductivity. Finally, we discuss metrological applications of the quantum Hall phenomenon.

I. INTRODUCTION

In a 2-dimensional electron system (2DES), Ohm's Law $\mathbf{J} = \sigma\mathbf{E}$ gives the relationship between the applied electric field and the induced current density at the level of linear response theory, where the conductivity σ is a rotationally-invariant 2×2 matrix of the form

$$\sigma = \begin{bmatrix} \sigma_{xx} & \sigma_{xy} \\ -\sigma_{xy} & \sigma_{xx} \end{bmatrix} . \tag{1}$$

The components σ_{xx}, σ_{xy} are referred to as the *longitudinal* and *Hall conductivities*, respectively. Remarkably, it is observed that, when a strong magnetic field is applied orthogonal to the plane of the 2DES (see schematic in Fig. 1(a)), the Hall conductivity varies stepwise with the strength of the magnetic field (see Fig. 1(b)), with plateaux at the universal quantized values

$$\sigma_{xy} = \frac{e\nu}{\Phi_0} , \qquad \nu \in \mathbb{N} . \tag{2}$$

where we have defined the fundamental constant $\Phi_0 = 2\pi\hbar/e$, known as the *flux quantum*. Moreover, the longitudinal conductivities vanish precisely on these plateaux (also seen in Fig. 1(b)), indicating the absence of longitudinal transport. This is the *(integer) quantum Hall effect* (QHE).

The observation that the Hall conductivity is exactly quantized as in equation (2) for any magnetic field strength was first realized experimentally by von Klitzing et al. [1]. Since then, a rich body of literature (see e.g. [2]) has developed to provide a theoretical foundation for this phenomenon, involving the confluence of a number of important concepts, such as the role of disorder in localizing quantum states, and the relevance of topological considerations. We elaborate upon these developments below, beginning with an elementary description of a single electron in the presence of a magnetic field.

II. THEORY

A. A First Approach: Landau Levels

The quantum Hamiltonian for a single particle in a magnetic field $\mathbf{B} = \nabla \times \mathbf{A} = B\,\hat{\mathbf{z}}$ is given by

$$\hat{H} = \frac{1}{2m_e}\big(\hat{\mathbf{p}} + e\mathbf{A}(\hat{x},\hat{y})\big)^2 , \tag{3}$$

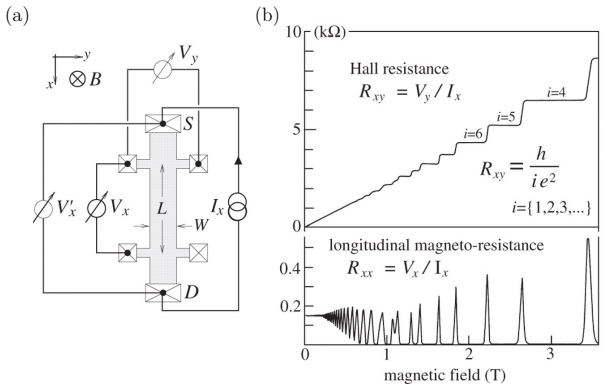

FIG. 1. (a) Schematic of a Hall bar apparatus, with orthogonal B-field; a current is applied in the y-direction, and the longitudinal (y-direction) and transverse (x-direction) voltage are measured. (b) Hall resistance R_{xy} and longitudinal resistance R_{xx} as a function of magnetic field strength; for the quantum Hall system, $\sigma_{xx} = 0$ if and only if R_{xx} vanishes, and $\sigma_{xy} = R_{xy}^{-1}$. Figure taken from [3].

where one has $\hat{\mathbf{p}} = -i\hbar\big(\partial_x, \partial_y\big)$ for a system constrained to the (x, y)-plane, and m_e and e are the electron mass and charge. It will be advantageous to use Landau gauge

$$\mathbf{A}(x, y) = xB\hat{\mathbf{y}} , \tag{4}$$

whereupon the Hamiltonian can be written as

$$\hat{H} = \frac{1}{2m_e}\Big(\hat{p}_x^2 + (\hat{p}_y + eB\hat{x})^2\Big) . \tag{5}$$

Evidently, the momentum p_y is a good quantum number, so we may investigate product eigenstates of the form

$$\psi_{k_y}(x, y) = e^{ik_y y} f_{k_y}(x) , \tag{6}$$

upon which the Hamiltonian acts as

$$\begin{aligned} \hat{H}\psi_{k_y} &= \frac{1}{2m_e}\Big(\hat{p}_x^2 + (\hbar k_y + eB\hat{x})^2\Big)\psi_{k_y} \\ &= \Big(\frac{\hat{p}_x^2}{2m_e} + \frac{m_e\omega_B^2}{2}\big(\hat{x} + k_y\ell_B^2\big)^2\Big)\psi_{k_y} , \end{aligned} \tag{7}$$

where we have recalled the expression $\omega_B = eB/m_e$ for the cyclotron frequency of an electron in a uniform magnetic field, and we have implicitly defined the *magnetic length* $\ell_B \equiv \sqrt{\hbar/eB}$. This is manifestly the Hamiltonian

for a 1-dimensional quantum harmonic oscillator (QHO) centred at $x = -k_y\ell_B^2$; if we define operators

$$\hat{a} = \frac{1}{\sqrt{2\hbar eB}}\big(\hat{p}_x - ieB\hat{x}\big)\,, \quad \hat{a}^\dagger = \frac{1}{\sqrt{2\hbar eB}}\big(\hat{p}_x + ieB\hat{x}\big)\,, \tag{8}$$

then we recover the typical QHO commutation relations, and we can implement the standard QHO analysis. The energy levels are $E_n = \hbar\omega_B\big(n + \frac{1}{2}\big)$, where $n \in \mathbb{N}$ is the eigenvalue of the number operator $\hat{\mathcal{N}} = \hat{a}^\dagger\hat{a}$. Consequently, if we neglect spin, then the operators $\hat{p}_y$ and $\hat{\mathcal{N}}$ form a complete set of commuting observables, and we can index all energy eigenstates $\psi_{n,k_y}(x,y)$ by the corresponding quantum numbers (n, k_y).

The eigenenergies of the system thus arrange themselves into highly degenerate *Landau levels* (LLs), indexed by the quantum number n, with the degeneracy corresponding to a continuum of possible momenta $\hbar k_y$. In reality, the Hall geometry has finite dimensions L_x, L_y, so the momenta must be quantized, and we expect a cut-off at large momenta, due to the non-zero lattice spacing within a given material; the degeneracy is thus large but finite. If we model the edges of the Hall sample with an 'infinite well' confining potential, then the y-momenta are quantized as $k_y \in \frac{2\pi}{L_y}\mathbb{N}$. Furthermore, since the eigenstates in a given LL are harmonic oscillator eigenstates centred at $x = -k_y\ell_B^2$, the restriction $|x| < L_x/2$ can be interpreted as a restriction $|k_y| < L_x/2\ell_B^2$ on allowed momenta. The degeneracy in a single LL is then roughly

$$N_{\mathrm{LL}} = \frac{L_y}{2\pi}\int_{-L_x/2\ell_B^2}^{L_x/2\ell_B^2} dk = \frac{L_xL_y}{2\pi\ell_B^2} = \frac{BL_xL_y}{\Phi_0}\,. \tag{9}$$

1. *From Landau Levels to the QHE*

In Section II C, a fully quantum mechanical treatment of the multi-particle QHE is given; however, our discussion of LLs already allows for an intuitive semi-classical derivation, following [4], in the case of integer *filling fraction* $\nu \equiv N/N_{\mathrm{LL}}$, interpreted as the number of filled LLs. One such derivation is found in Appendix B, where we assume a large sample, so that edge effects may be neglected; it is seen that an applied electric field lifts the degeneracy in each LL, and one recovers the correct expression for the conductivities. In reality, one cannot neglect edge effects; in fact, the physics of the near-edge region is essential to an understanding of the QHE. We will therefore introduce an approximately U-shaped confining potential $V(x)$, as depicted in Fig. 2(a), with a steep incline near the edges of the sample in the x-direction; one has

$$eV_{\mathrm{H}} = V(x_+) - V(x_-)\,, \tag{10}$$

where $x_\pm$ are the positions of the edges, and V_{H} is the applied Hall voltage. In the previous section, the degeneracy in a single Landau level was indexed by momentum

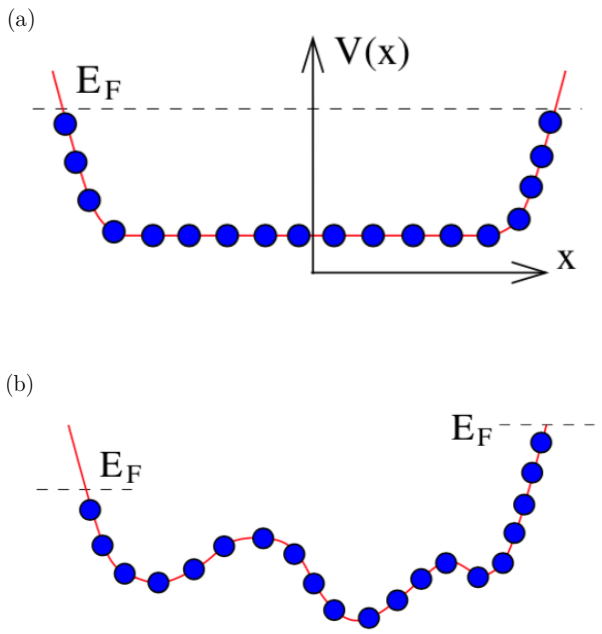

FIG. 2. (a) U-shaped confining potential; dots represent states localized around a given x-position. (b) Deformation of the U-shaped potential, due to applied voltage and impurities. Figures taken from [4].

k_y, or equivalently, by the equilibrium position $-k_y\ell_B^2$ of the state in the x-direction; the eigenstates continue to be localized in the x-direction in the presence of a uniform electric field. We may therefore assume that the effect of the confining potential is to increase the energy associated with the states localized near the edge, which are referred to as *edge states* or *edge modes*, as depicted in Fig. 2(a). (The unperturbed energy eigenstates localized in the bulk are strongly suppressed near the edges if $\ell_B \ll L_x$, so the confining potential only slightly deforms these states.)

If the potential can be approximated as linear in the vicinity of the edges, so that

$$V(x) \approx \frac{\partial V}{\partial x}\Big|_{x=x_\pm}(x - x_\pm)\,, \tag{11}$$

then one might classically anticipate that an electron localized near the edges should have velocity

$$\mathbf{v} = -\frac{1}{eB}\frac{\partial V}{\partial x}\Big|_{x=x_\pm}\hat{\mathbf{y}}\,, \tag{12}$$

since this satisfies the Lorentz force law; for a single electron, this should also hold quantum mechanically by Ehrenfest's theorem. That is, the edge states result in an effectively 1-dimensional current flowing at the edge of the material, as though a wire were placed along the periphery of the sample; since the current flows in one direction, the edge states are said to be *chiral*.

If precisely an integer number $\nu \in \mathbb{N}$ of LLs is filled with non-interacting electrons, then the induced current

is seen to be

$$\mathbf{I} \approx -\nu e \int \frac{dk_y}{2\pi}\, \mathbf{v}_y(k_y) = \frac{\nu}{2\pi B}\int \frac{dx}{\ell_B^2}\frac{\partial V}{\partial x}\hat{\mathbf{y}} = \frac{e\nu V_{\mathrm{H}}}{\Phi_0}\hat{\mathbf{y}}\,, \tag{13}$$

from which we may immediately deduce the desired conductivity in equation (2). We note that, as seen from the above computation, the conductivity is actually insensitive to the precise form of the potential in the interior, provided that the potential is sufficiently weak in the interior that the only states near the Fermi energy are edge states (see Fig. 2(b)). This illustrates the crucial role played by the edge states in charge transport; moreover, this invariance to small variations in the potential will be of particular interest in the next section, where we consider the role of disorder.

B. Hall Plateaux and the Role of Disorder

So far, our analysis has only been applicable to the case of integer filling fractions, and is thus unable to account for the plateaux in the values of the Hall conductivity that are observed as the magnetic field is varied. The ingredient missing from the above discussion is the vital role played by the impurities present in a realistic system.

Disorder in a system can be modelled by adding a small, random electronic potential to the Hamiltonian; in a quantum Hall system, provided that this random potential is much smaller than the energy associated with the electronic cyclotron motion, this can be treated in perturbation theory. The disorder potential then leads to splitting in the highly degenerate Landau levels, so that the density of states, previously δ-function localized to the LL energies, becomes broader and turns into bands, as shown in Fig. 3(a). Between these bands reside only the edge states, whose energies deviate significantly from the LL energies.

The way in which disorder induces Hall plateaux, however, is through the mechanism of *localization*, wherein quantum states are restricted to small regions of the total system, rather than diffusing throughout the system. The genericity of localization in the presence of disorder is a well-studied phenomenon (see e.g. [5–9]), including in the case of the QHE [10]; most notably, in the celebrated tight-binding model

$$H = -t\sum_{\langle m,n\rangle} c_m^\dagger c_n + \sum_n U_n c_n^\dagger c_n \tag{14}$$

of Anderson [5], with constant hopping t and on-site terms U_n which are i.i.d. random variables in some fixed range $U_n \in [-W, W]$, the energy eigenstates are found to be *localized states* of the form

$$|\psi(\mathbf{r})|^2 \sim e^{-|\mathbf{r}-\mathbf{r}_0|/\xi} \tag{15}$$

in the thermodynamic limit $n \to \infty$, provided that W is larger than some critical value W_{c}. Here, ξ is understood

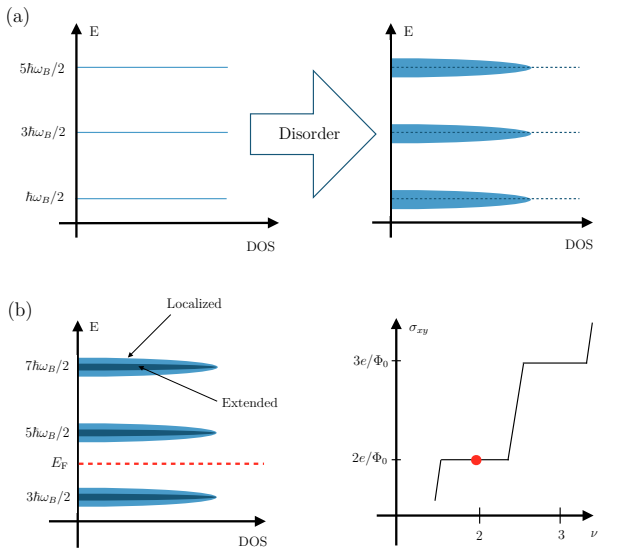

FIG. 3. (a) Broadening of Landau levels due to microscopic disorder. (b) States at the edges of the Landau bands are localized, whereas states in the centre are extended; if the Fermi energy lies between bands, then the conductivity lies on a plateaux.

to represent the correlation length of such a state, giving a characteristic length scale for the distribution of the wavefunction. In the limite $\xi \to \infty$, the state becomes an *extended state*.

In the quantum Hall system, there is another way to analyze the localization effect. Recall that a classical electron in a magnetic field undergoes cyclotron motion

$$\begin{aligned} x(t) &= x_0 - R\sin(\omega_B t + \phi) = x_0 + \frac{\dot{y}(t)}{\omega_B} \\ y(t) &= y_0 + R\cos(\omega_B t + \phi) = y_0 - \frac{\dot{x}(t)}{\omega_B}\,; \end{aligned} \tag{16}$$

one may therefore argue that the quantized versions of the 'centre position' variables x_0, y_0 are given by

$$\hat{x}_0 = \hat{x} - \frac{1}{\omega_B}\frac{d}{dt}\hat{y}\,, \quad \hat{y}_0 = \hat{y} + \frac{1}{\omega_B}\frac{d}{dt}\hat{x}\,, \tag{17}$$

whence one finds from the Schrödinger equation, and the canonical commutation relations for $\hat{x}, \hat{y}$ and their derivatives, that

$$i\hbar\dot{\hat{x}}_0 = i\ell_B^2\frac{\partial V(\hat{x},\hat{y})}{\partial y_0}\,, \quad i\hbar\dot{\hat{y}}_0 = -i\ell_B^2\frac{\partial V(\hat{x},\hat{y})}{\partial x_0}\,. \tag{18}$$

Thus, in expectation value, a single electron moves along equipotential contours. Generically, the equipotential contours of a random potential will be closed orbits; consequently, an electron restricted to move along such a contour will be bound to a small region, whose size is comparable to the distance between impurities. In particular, the states that are most localized are those restricted to equipotentials contours near the peaks and

troughs of the disorder potential, which are also at the upper and lower edges of the Landau band (see Fig. 3(b)).

The relevance of the localization phenomenon comes from the fact that, to a first approximation, a localized state does not transport charge, and therefore does not contribute to the current. If the Fermi level lies within the region of extended states, then the conducting electrons can move freely, as in a metal. However, if we increase the electron density in the system or reduce the magnetic field, so that the Fermi level lies within the region of localized states, we do not gain any current-carrying states (and the material is said to be an *Anderson insulator*); therefore, the conductivity remains the same, a fact which is responsible for the plateaux observed over a broad range of filling fractions ν (see Fig. 3(b)). The region between the bands of extended states is referred to as a *mobility gap*. The precise role of disorder in Hall quantization is made manifest in a classic argument due to Laughlin [11]; a presentation of this argument can be found in Appendix D.

C. QHE from Topology

Insensitivity of the QHE to deformations of the system may be recognized as evidence that this effect is topological in origin. In the following, we will give a schematic argument [12] that the Hall conductivity σ_{xy} is an example of a topological invariant known as a *TKNN invariant*. We draw upon the discussion from [4, 13, 14].

Consider a particle on a rectangular lattice, with lattice constants a_x, a_y, and general lattice vectors

$$\mathbf{R}_{mn} = ma_x\hat{\mathbf{x}} + na_y\hat{\mathbf{y}}\,, \qquad m,n \in \mathbb{Z}. \tag{19}$$

The primitive lattice vectors for the reciprocal lattice are evidently $\mathbf{b}_1 = \frac{2\pi}{a_x}\hat{\mathbf{x}}$, $\mathbf{b}_2 = \frac{2\pi}{a_y}\hat{\mathbf{y}}$, and the first Brillouin zone is simply the region $\mathbf{k} \in [-\frac{\pi}{a_x}, \frac{\pi}{a_x}) \times [-\frac{\pi}{a_y}, \frac{\pi}{a_y})$. Invariance of the Hamiltonian H to lattice translations implies that we have energy eigenstates of the Bloch form

$$\psi_{\mathbf{k}}(\mathbf{x}) = u_{\mathbf{k}}(\mathbf{x})e^{i\mathbf{k}\cdot\mathbf{x}}\,,$$
$$u_{\mathbf{k}}(\mathbf{x} + a_x\hat{\mathbf{x}}) = u_{\mathbf{k}}(\mathbf{x} + a_y\hat{\mathbf{y}}) = u_{\mathbf{k}}(\mathbf{x})\,.$$

We thus have effective momentum-dependent Hamiltonian $H_{\mathbf{k}} = e^{-i\mathbf{k}\cdot\mathbf{x}}He^{i\mathbf{k}\cdot\mathbf{x}}$ such that $H_{\mathbf{k}}|u_{\mathbf{k}}\rangle = E_{\mathbf{k}}|u_{\mathbf{k}}\rangle$. It is then natural to define the current operator to be the charge multiplied by the 'group velocity' operator for a wavepacket of Bloch eigenstates; namely, we define

$$\mathbf{J} = e \times \frac{1}{\hbar}\frac{\partial H_{\mathbf{k}}}{\partial \mathbf{k}}\,. \tag{20}$$

Suppose that the Hamiltonian for the system neglects electron-electron interactions, and that the Fermi energy E_F lies in a gap between bands; in reality, we have seen that the latter condition should actually refer to a mobility gap. In Appendix E, the Kubo formula

$$\sigma_{xy} = i\hbar\sum_{n\neq m}\frac{\langle m|J_y|n\rangle\langle n|J_x|m\rangle - \langle m|J_x|n\rangle\langle n|J_y|m\rangle}{(E_n - E_m)^2}\,. \tag{21}$$

for the conductivity in the energy eigenstate $|m\rangle$ of a quantum mechanical system was derived, where $|n\rangle$ are eigenstates of the Hamiltonian with energy eigenvalues E_n. This formula must be somewhat modified to describe the conductivity in the many-body ground state; using the current defined in equation (20), the appropriate reformulation for our purposes is

$$\sigma_{xy} = \frac{ie^2}{\hbar}\sum_{E_\alpha<E_F<E_\beta}\int\frac{d^2\mathbf{k}}{(2\pi)^2}\frac{d^2\mathbf{k}'}{(2\pi)^2}\,\mathcal{S}(u^\alpha_{\mathbf{k}}, u^\beta_{\mathbf{k}'})\,, \tag{22}$$

where

$$\begin{aligned}\mathcal{S}(u^\alpha_{\mathbf{k}}, u^\beta_{\mathbf{k}'}) = &\frac{\langle u^\alpha_{\mathbf{k}}|\frac{\partial H_{\mathbf{k}}}{\partial k^y}|u^\beta_{\mathbf{k}'}\rangle\langle u^\beta_{\mathbf{k}'}|\frac{\partial H_{\mathbf{k}}}{\partial k^x}|u^\alpha_{\mathbf{k}}\rangle}{(E_\beta(\mathbf{k}') - E_\alpha(\mathbf{k}))^2}\\ &- \frac{\langle u^\alpha_{\mathbf{k}}|\frac{\partial H_{\mathbf{k}}}{\partial k^x}|u^\beta_{\mathbf{k}'}\rangle\langle u^\beta_{\mathbf{k}'}|\frac{\partial H_{\mathbf{k}}}{\partial k^y}|u^\alpha_{\mathbf{k}}\rangle}{(E_\beta(\mathbf{k}') - E_\alpha(\mathbf{k}))^2}\,.\end{aligned} \tag{23}$$

Here, the integrals are over the Brillouin zone, while the sum is over pairs of states $u^\beta_{\mathbf{k}'}, u^\alpha_{\mathbf{k}}$ above and below the Fermi energy respectively. A simple manipulation employing the completeness relation

$$\sum_\beta\int\frac{d^2\mathbf{k}'}{(2\pi)^2}|u^\beta_{\mathbf{k}'}\rangle\langle u^\beta_{\mathbf{k}'}| = 1 - \sum_\alpha\int\frac{d^2\mathbf{k}}{(2\pi)^2}|u^\alpha_{\mathbf{k}}\rangle\langle u^\alpha_{\mathbf{k}}| \tag{24}$$

then yields

$$\sigma_{xy} = \frac{ie^2}{\hbar}\sum_{E_\alpha<E_F}\int\frac{d^2\mathbf{k}}{(2\pi)^2}\left[\langle\frac{\partial u^\alpha_{\mathbf{k}}}{\partial k^y}|\frac{\partial u^\alpha_{\mathbf{k}}}{\partial k^x}\rangle - \langle\frac{\partial u^\alpha_{\mathbf{k}}}{\partial k^x}|\frac{\partial u^\alpha_{\mathbf{k}}}{\partial k^y}\rangle\right]. \tag{25}$$

We would like to use the Kubo formula to relate the Hall conductivity to a fundamental topological invariant of the system. To this end, we define the quantity

$$\mathcal{A}_j(\alpha,\mathbf{k}) = -i\langle u^\alpha_{\mathbf{k}}|\frac{\partial}{\partial k^j}|u^\alpha_{\mathbf{k}}\rangle\,; \tag{26}$$

it can be seen that this is nothing other than an Abelian connection over the Brillouin zone for the band α, a so-called *Berry connection*, analogous to the gauge field of classical electromagnetism. In particular, we see that under a local phase shift of the Bloch states $u_{\mathbf{k}} \to e^{i\omega(\mathbf{k})}u_{\mathbf{k}}$ with $\omega(\mathbf{k})$ a generic smooth function, one has

$$\mathcal{A}_j(\alpha,\mathbf{k}) \to \mathcal{A}_j(\alpha,\mathbf{k}) + \frac{\partial\omega}{\partial k^j}\,, \tag{27}$$

the expected behaviour for a connection under a $U(1)$ gauge transformations. The curvature tensor corresponding to this connection is

$$\begin{aligned}\mathcal{F}_{ij}(\alpha) &= \frac{\partial\mathcal{A}_j(\alpha,\mathbf{k})}{\partial k^i} - \frac{\partial\mathcal{A}_i(\alpha,\mathbf{k})}{\partial k^j}\\ &= -i\langle\frac{\partial u^\alpha_{\mathbf{k}}}{\partial k^i}|\frac{\partial u^\alpha_{\mathbf{k}}}{\partial k^j}\rangle + i\langle\frac{\partial u^\alpha_{\mathbf{k}}}{\partial k^j}|\frac{\partial u^\alpha_{\mathbf{k}}}{\partial k^i}\rangle\,,\end{aligned} \tag{28}$$

so we see instantly that

$$\sigma_{xy} = \frac{e^2}{\hbar} \sum_\alpha \int \frac{dk^x dk^y}{(2\pi)^2} \mathcal{F}_{xy}(\alpha) \,. \tag{29}$$

By an extension of the Gauss-Bonnet theorem, the integral of the Berry curvature $\mathcal{F}_{xy}(\alpha)$ over the Brillouin zone is $2\pi C_\alpha$, with C_α an exact integer, referred to as the *Chern number*. We thus recover Hall quantization

$$\sigma_{xy} = \frac{e^2}{2\pi\hbar} \sum_\alpha C_\alpha \in \frac{e^2}{2\pi\hbar} \mathbb{Z} \,. \tag{30}$$

This argument reveals something deep about the importance of *topological order* in determining the properties of a material.

III. EXPERIMENTAL REALIZATIONS

Experimental probing of the QHE was instigated in [15], where the Hall conductivity was measured for the 2-dimensional electron gas (2DEG) formed in a MOS inversion layer (c.f. below). Similar techniques were subsequently employed in the seminal work of von Klitzing [1], where the QHE plateaux of Fig. 1 were first observed; this work was honoured with the Nobel Prize in physics in 1985. Even though some aspects of the QHE, such as the vanishing of the longitudinal resistance, had been known prior to the work of von Klitzing [15, 16], the quantized Hall resistance had not been theoretically anticipated. As discussed above, this discovery heralded the pervasive role of topology in condensed matter physics, which remains and active area of research (e.g. in studies of the fractional Hall effect and the quantum spin Hall effect). In the following, we provide some experimental details regarding the von Klitzing experiment; more recent experimental investigations involving graphene systems include [17, 18] (see Appendix F).

A. 2DEG in the inversion layer of a MOSFET

The main experimental challenge in observing the QHE is the manufacture of a 2DEG, whose transport properties in the presence of a magnetic field may then be probed. This can be realized using a quantum well with width comparable to the de Broglie wavelength of the electron. This splits the energy spectrum into distinct subbands; at sufficiently low temperatures, only the lowest energy subband is occupied, and the electrons are effectively confined to 2 dimensions. In [1], the n-type inversion layer of a Metal-Oxide-Semiconductor-Field-Effect-Transistor (MOSFET) was used (see schematic in Fig. 4). A metallic gate electrode is located above the p-type silicon substrate, which is electrically insulated by an SiO_2 layer. This setup allows the charge carrier density of the inversion layer to be adjusted by varying the gate voltage.

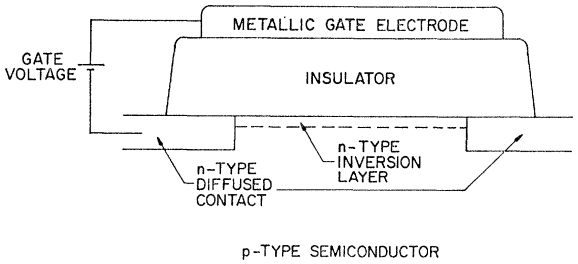

FIG. 4. Schematics of a metal-insulator-semiconductor structure, with an n-type inversion layer as 2DEG. The traditional MOSFET uses silicon as substrate and SiO_2 as insulator [19].

Fig. 5 shows the MOSFET band diagram near the surface of the substrate. The z-axis is chosen to be perpendicular to the device, starting at the substrate-insulator interface ($z = 0$ Å) and going deeper into the substrate for increasing z-values. Band-bending is observed at the junction; the lower edge of the conduction band E_c is at a minimum near the substrate-insulator interface, with precise shape determined by the gate voltage. The curve $g(z)$ represents the charge carrier density for electrons in the lowest energy subband E_0, which becomes localized at the interface, leading to the 2DEG [19]. The energies E_1 and E_2 of higher subbands are also shown.

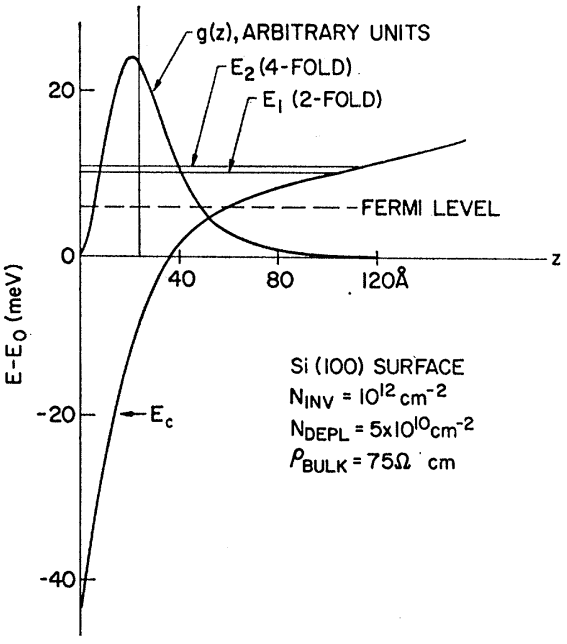

FIG. 5. Potential well (E_c) near the substrate-insulator interface ($z = 0$ Å). The charge carrier density $g(z)$ of the lowest subband E_0 has a maximum near the surface, resulting in the 2DEG [19].

1. The Hall Bar and Four-Terminal Measurement

In order to accurately determine the longitudinal and transverse resistances, one needs to perform a precise measurement of both the current and voltage in the Hall bar system. Starting with the longitudinal resistance, one could imagine applying the simple setup of Fig. 6(a). The 2DEG is connected with two ohmic contacts to a voltage supply U and the current meter I. The equivalent circuit in Fig. 6(b) shows the additional measured resistances of the current meter R_{iC}, the powersupply R_{iV} and the two contacts R_{contacts}, which would lead to inaccurate measurement results. A much improved result can be achieved by using the so called *four-terminal measurement* seen in Fig. 6(c). Here, the voltage supply is changed to a current source I, which drives a constant current through the 2DEG. A high impedance-voltmeter V is used to measure the longitudinal voltage drop of the 2DEG. Its contacts (Fig. 6(d)) have ideally no voltage drop due to the high impedance measurement.

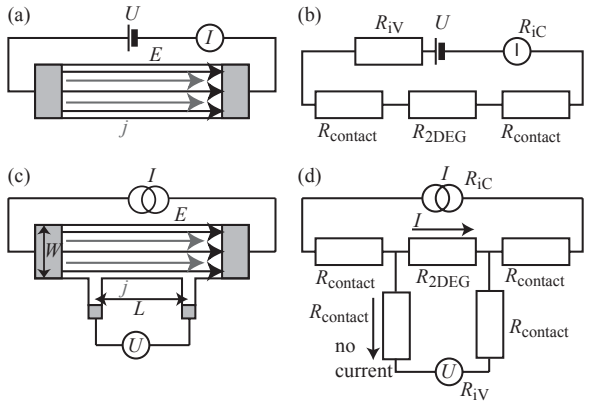

FIG. 6. (a) Two-terminal measurement for a 2DEG. (b) Equivalent circuit showing the additional measured resistances, which lead to inaccurate results. (c) Four-terminal measurement. (d) Equivalent circuit which allows the resistance measurement of only the 2DEG [20].

For the measurement of the transverse Hall resistance, one adds two additional contacts on the transverse edges of the 2DEG (as seen in Fig. 1), leading to the typical Hall bar geometry. Using the same principle, one achieves reasonably good values for the Hall voltage drop and the Hall resistance.

IV. APPLICATIONS

The robustness of the Hall quantization to microscopic disorder and changes in the macroscopic properties of a material makes the measurement of the Hall conductivity an appealing metrological standard. The relation between the fine structure constant α and the von Klitzing constant R_K is given by

$$R_K \equiv \frac{2\pi\hbar}{e^2} = \frac{\mu_0 c}{2\alpha}\,. \tag{31}$$

In SI, the vacuum permeability μ_0 and the speed of light are fixed constants; thus, the fine structure constant can be inferred directly from a measurement of R_K. The operative impediments to this method are then limitations in how well the precision of a reference resistor can be maintained. At present, two electrical units need to be realized in terms of the metre and the kilogram in order to make electrical units measurable in the SI. Generally, the ohm (Ω) and the watt (W) are chosen, as these units can be most accurately determined experimentally [21]. Due to a theorem of Thompson and Lampard [22], the capacitance of a particular class of capacitor can be related to a single length measurement. With this calculable capacitance, the resistance of a resistor can be determined through bridge techniques [23], with a precision of up to 1 part in 10^8, about two orders of magnitude less precise than the reproducibility of the von Klitzing constant. Finally, a DC current comparator bridge may be used to determine R_K relative to the reference resistance. This procedure constitutes the second most accurate method for the determination of α; the most accurate involves comparing the experimentally observed anomalous magnetic moment a_e of the electron to the famous QED prediction, evaluated up to tenth order in [24].

Historically, the QHE has also been used to define the SI unit of resistance, from which all other electric units must be derived. However, this definition is likely to be abrogated during the revision of the International System of Units, to take place in early 2019, wherein fixed values will be assigned to seven physical constants, including the Planck constant and the elementary charge, thereby making the von Klitzing constant a defined quantity (see Appendix G for further discussion).

[1] K. v. Klitzing, G. Dorda, and M. Pepper. New method for high-accuracy determination of the fine-structure constant based on quantized Hall resistance. *Phys. Rev. Lett.*, 45(6):494–497, 1980.

[2] R. E. Prange and S. M. Girvin. *The Quantum Hall Effect*. Graduate texts in contemporary physics. Springer-Verlag, 1987. ISBN 9783540962861.

[3] J. Weis and K. von Klitzing. Metrology and microscopic picture of the integer quantum Hall effect. *Phil. Trans. R. Soc.*, 369:3954–3974, 2011. doi:10.1098/rsta.2011.0198.

[4] David Tong. The Quantum Hall Effect. `http://www.damtp.cam.ac.uk/user/tong/qhe.html`, January 2016.

[5] P. W. Anderson. Absence of diffusion in certain random lattices. *Phys. Rev.*, 109(5):1492–1505, 1958.

[6] E. Abrahams, P. W. Anderson, D. C. Licciardello, and T. V. Ramakrishnan. Scaling theory of localization: Absence of quantum diffusion in two dimensions. *Phys. Rev. Lett.*, 42(10):673–676, 1979.

[7] J. T. Edwards and D. J. Thouless. Numerical studies of localization in disordered systems. *J. Phys. C: Solid State Phys.*, 5(8):807–820, 1972.

[8] D. Vollhardt and P. Wölfle. Scaling equations from a self-consistent theory of anderson localization. *Phys. Rev. Lett.*, 48(10):699–702, 1982.

[9] D. M. Basko, I. L. Aleiner, and B. L. Altshuler. Metal-insulator transition in a weakly interacting many-electron system with localized single-particle states. *Ann. Phys.*, 321(5):1126–1205, 2006.

[10] A. M. M. Pruisken. Universal singularities in the integral quantum Hall effect. *Phys. Rev. Lett.*, 61(11):1297–1300, 1988.

[11] R. B. Laughlin. Quantized Hall conductivity in two dimensions. *Phys. Rev. B*, 23(10):5632–5633, 1981.

[12] M. P. Nightingale D. J. Thouless, M. Kohmoto and M. den Nijs. Quantized Hall conductance in a two-dimensional periodic potential. *Phys. Rev. Lett.*, 49(6): 405–408, 1982.

[13] J. K. Jain. *Composite Fermions*, chapter 2-4. Cambridge University Press, 2007. ISBN 9780511607561.

[14] Eduardo Fradkin. *Field Theories of Condensed Matter Physics*, chapter 12. Cambridge University Press, 2013. ISBN 9781139015509.

[15] S.Kawaji and J.Wakabayashi. Quantum galvanomagnetic properties of n-type inversion layers on Si(100) MOSFET. *Surface Science*, 58(1):238–245, 1976.

[16] Jun ichi Wakabayashi. Hall effect in silicon MOS inversion layers under strong magnetic fields. *J. Phys. Soc. Jpn.*, 44(6):1839–1849, 1978.

[17] Yuanbo Zhang, Tan Yan-Wen, Horst L. Stormer, and Philip Kim. Experimental observation of the quantum Hall effect and Berry's phase in graphene. *Nature*, 438 (7065):201–204, 2005.

[18] T. Shen, J. J. Gu, M. Xu, Y. Q. Wu, M. L. Bolen, M. A. Capano, L. W. Engel, and P. D. Ye. Observation of quantum-Hall effect in gated epitaxial graphene grown on SiC (0001). *Applied Physics Letters*, 95(17):172105, October 2009. doi:10.1063/1.3254329.

[19] Frank Stern and W. E. Howard. Properties of semiconductor surface inversion layers in the electric quantum limit. *Phys. Rev.*, 163:816–835, Nov 1967. doi: 10.1103/PhysRev.163.816. URL `https://link.aps.org/doi/10.1103/PhysRev.163.816`.

[20] Thomas Ihn. *Semiconductor nanostructures: quantum states and electronic transport*. Oxford Univ. Press, 2010. ISBN 9780199534425. doi:10.1093/acprof:oso/9780199534425.001.0001. URL `http://dx.doi.org/10.1093/acprof:oso/9780199534425.001.0001`.

[21] B. Jeckelmann and B. Jeanneret. The Quantum Hall Effect as an Electrical Resistance Standard. *Séminaire Poincaré*, 2:39–51, 2004.

[22] A.M. Thompson and D.G. Lampard. A New Theorem in Electrostatics and its Application to Calculable Standards of Capacitance. *Nature (London)*, 177:888, 1956.

[23] A Jeffery, R E Elmquist, J Q Shields, L H Lee, M E Cage, S H Shields, and R F Dziuba. Determination of the von Klitzing constant and the fine-structure constant through a comparison of the quantized Hall resistance and the ohm derived from the NIST calculable capacitor. *Metrologia*, 35(2):83–96, 1998. doi:10.1088/0026-1394/35/2/3.

[24] Tatsumi Aoyama, Masashi Hayakawa, Toichiro Kinoshita, and Makiko Nio. Tenth-Order QED Contribution to the Electron g-2 and an Improved Value of the Fine Structure Constant. *Phys. Rev. Lett.*, 109:111807, 2012. doi:10.1103/PhysRevLett.109.111807.

[25] B. I. Halperin. Quantized Hall conductance, current-carrying edge states, and the existence of extended states in a two-dimensional disordered. *Phys. Rev. B*, 25(4): 2185–2190, 1982.

[26] M. Peskin and D. Schroeder. *An Introduction to Quantum Field Theory*, chapter 4. Perseus Books, 1995.

[27] K. S. Novoselov, A. K. Geim, S. V. Morozov, D. Jiang, Y. Zhang, S. V. Dubonos, I. V. Grigorieva, and A. A. Firsov. Electric Field Effect in Atomically Thin Carbon Films. *Science*, 306:666–669, 2004.

[28] G. W. Semenoff. Condensed-matter simulation of a three-dimensional anomaly. *Phys. Rev. Lett.*, 53(26):2449–2452, 1984.

[29] Ahmed Abouelsaood. Relation between the Chiral Anomaly and the Quantized Hall Effect. *Phys. Rev. Lett.*, 54(18):1973–1975, 1985.

[30] F. D. M. Haldane. Model for a Quantum Hall Effect without Landau Levels: Condensed-Matter Realization of the "Parity Anomaly". *Phys. Rev. Lett.*, 61(18):2015–2018, 1988.

[31] B. A. Bernevig, T. L. Hughes, and S.-C. Zhang. The quantum Hall effect in graphene from a lattice perspective. *Solid State Comm.*, 143:20–26, 2007.

[32] Klaus von Klitzing. The quantized Hall effect. *Rev. Mod. Phys.*, 58:519–531, Jul 1986. doi: 10.1103/RevModPhys.58.519. URL `https://link.aps.org/doi/10.1103/RevModPhys.58.519`.

[33] F. Delahaye. Technical Guidelines for Reliable Measurements of the Quantized Hall Resistance. *Metrologia*, 26 (1):63–68, 1989. doi:10.1088/0026-1394/26/1/005.

[34] Bureau International des Poids et Mesures. Proceedings of the 24th meeting of the General Conference on Weights and Measures. 2011. URL `https://www.bipm.org/utils/common/pdf/CGPM/CGPM24.pdf`.

Appendix A: Classical Hall Effect

At the classical level, one can analyze the Hall effect by considering the average motion of a single electron in a Hall bar geometry with orthogonal magnetic field $\mathbf{B} = B\hat{\mathbf{z}}$ and in-plane electric field $\mathbf{E} = E\hat{\mathbf{x}}$. The Lorentz force law, modified by a Drude model-type friction term, gives

$$m_e \frac{d}{dt}\langle \mathbf{v} \rangle = -e\big(\mathbf{E} + \langle \mathbf{v} \rangle \times \mathbf{B}\big) - \frac{m}{\tau}\langle \mathbf{v} \rangle \,, \tag{A1}$$

where $\langle \mathbf{v} \rangle$ is an ensemble average for the electron velocity, m_e is the electron mass, and τ is the mean free time. At equilibrium, $\frac{d}{dt}\langle \mathbf{v} \rangle = 0$, so the above yields

$$\begin{aligned} 0 &= -eE_x - eB\langle v_y \rangle - \frac{m}{\tau}\langle v_x \rangle \\ 0 &= -eE_y + eB\langle v_x \rangle - \frac{m}{\tau}\langle v_y \rangle \,, \end{aligned} \tag{A2}$$

that is,

$$e\begin{bmatrix}E_x\\E_y\end{bmatrix} = -\begin{bmatrix}m/\tau & eB\\ -eB & m/\tau\end{bmatrix}\begin{bmatrix}\langle v_x\rangle\\ \langle v_y\rangle\end{bmatrix} . \tag{A3}$$

Given that the current is $\mathbf{J} = -ne\langle\mathbf{v}\rangle$, we have immediately that

$$\mathbf{E} = \frac{1}{ne^2}\begin{bmatrix}m/\tau & eB\\ -eB & m/\tau\end{bmatrix}\mathbf{J} \equiv \rho\mathbf{J} . \tag{A4}$$

We have therefore found longitudinal and Hall resistivities

$$\rho_{xx} = \frac{m}{ne^2\tau} , \qquad \rho_{xy} = \frac{B}{ne} = \frac{m\omega_B}{ne^2} , \tag{A5}$$

where $\omega_B = eB/m$ denotes the typical cyclotron frequency for an electron in a uniform magnetic field. Note that the Hall resistivity varies linearly with the magnetic field B in the classical case, rather than stepwise.

Appendix B: Landau Levels with Constant Electric Field and the QHE

The analysis of a single electron in the presence of a magnetic field, discussed in Section II A, may be repeated with the addition of an in-plane electric field $\mathbf{E} = E\hat{\mathbf{x}}$, implemented through electrostatic potential energy term $\Phi(x, y) = -Ex$. The Hamiltonian is thus modified to

$$\hat{H} = \frac{1}{2m_e}\big(\hat{p}_x^2 + (\hat{p}_y + eB\hat{x})^2\big) - eE\hat{x} . \tag{B1}$$

The momentum p_y is still a good quantum number, so we can again consider product eigenstates as in equation (6), upon which the Hamiltonian acts as

$$\begin{aligned}\hat{H}\psi_{k_y} &= \Big[\frac{1}{2m_e}\Big(\hat{p}_x^2 + (\hbar k_y + eB\hat{x})^2\Big) - eE\hat{x}\Big]\psi_{k_y}\\ &= \Big[\frac{\hat{p}_x^2}{2m_e} + \frac{m_e\omega_B^2}{2}\big(\hat{x} + k_y\ell_B^2 - \frac{m_eE}{eB^2}\big)^2\Big]\psi_{k_y}\\ &\quad + \Big[\frac{\hbar k_yE}{B} - \frac{mE^2}{2B^2}\Big]\psi_{k_y} .\end{aligned} \tag{B2}$$

This is now a QHO Hamiltonian with a trivial offset in the energy; the energy eigenvalues are then

$$E_{n,k_y} = \hbar\omega_B^2\big(n + \frac{1}{2}\big) + \frac{\hbar E}{B}k_y - \frac{mE^2}{2B^2} , \tag{B3}$$

which breaks the degeneracy in each LL.

We can use the above to derive the QHE for the case of integer filling fraction ν, so that the Fermi energy E_F lies between Landau levels. We assume that the sample is sufficiently large that edge effects can be neglected; the applied Hall voltage then manifests as a uniform electric field $\mathbf{E} = E\hat{\mathbf{x}}$ throughout the sample, the scenario that we have just analyzed. (In reality, the electrostatic potential within the bulk will not be exactly linear, due to impurities and edge effects; see Fig. 7.) Hamilton's equations yield $m_e\dot{\mathbf{x}} = \mathbf{p} + e\mathbf{A}$, and the sensible single-electron current operator is $\hat{\mathbf{I}} = -e\hat{\dot{\mathbf{x}}}$; in second quantization, this becomes

$$\hat{\boldsymbol{\mathcal{I}}} = -\frac{e}{m_e}\sum_{n,k_y}\langle\psi_{n,k_y}|\big(-i\hbar\boldsymbol{\nabla} + e\mathbf{A}\big)|\psi_{n,k_y}\rangle c^\dagger_{n,k_y}c_{n,k_y} , \tag{B4}$$

where we have obviously continued to neglect spins. In Landau gauge, we must therefore evaluate expectation values

$$-i\hbar\langle\psi_{n,k_y}|\partial_x|\psi_{n,k_y}\rangle , \quad -i\hbar\langle\psi_{n,k_y}|\Big(\partial_y + \frac{ieB\hat{x}}{\hbar}\Big)|\psi_{n,k_y}\rangle . \tag{B5}$$

The first quantity vanishes, since the momentum expectation value in an eigenstate of a QHO is zero. The latter yields

$$\hbar k_y - eB\Big(k_y\ell_B^2 + \frac{m_eE}{eB^2}\Big) = \frac{m_eE}{B} , \tag{B6}$$

given that the QHO states are centred at $-k_y\ell_B^2 + \frac{m_eE}{eB^2}$.

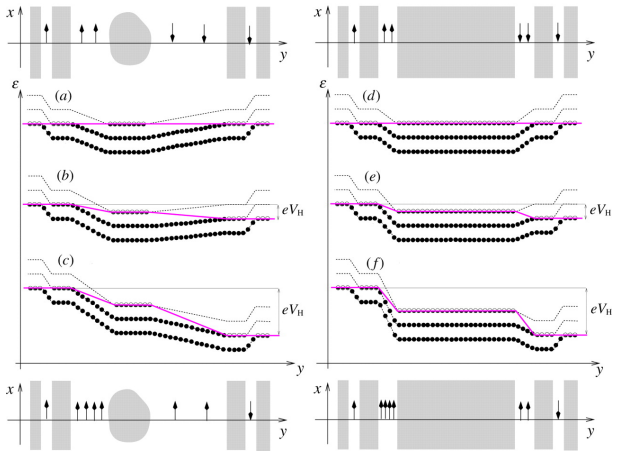

FIG. 7. Approximate bending of Landau levels in a 2DES. In each diagram, the pink curve represents the Hall potential. The upper and lower insets illustrate the differentiation between compressible and incompressible regions. Diagrams (a) and (d) illustrate the case of a 2DES in thermal equilibrium, diagrams (b) and (e) the case of a small applied Hall voltage, and diagrams (c) and (f) the case of a large applied Hall voltage. Figure taken from [3].

If we neglect electron-electron interactions, then the many-body ground state is simply a Slater determinant of the eigenstates ψ_{n,k_y} such that $n \in \{1, 2, \ldots, \nu\}$. The expectation value for the current operator is then

$$\begin{aligned}\langle\mathrm{GS}|\hat{\boldsymbol{\mathcal{I}}}|\mathrm{GS}\rangle &= -\frac{e}{m_e}\hat{\mathbf{y}}\sum_{n=1}^{\nu}\sum_{k_y}\Big(\frac{m_eE}{B}\Big)\\ &= -\frac{e\nu}{\Phi_0}EL_xL_y\hat{\mathbf{y}}\end{aligned} \tag{B7}$$

where we have used the result of equation (9) (neglecting spin degeneracy). It follows that the expectation for the current density is $\hat{\mathcal{J}}_x = 0$, $\hat{\mathcal{J}}_y = -eE\nu/\Phi_0$, from which we may deduce the desired conductivities

$$\sigma_{xx} = 0\,, \qquad \sigma_{xy} = \frac{e\nu}{\Phi_0}\,. \tag{B8}$$

In addition to eliding the role of edge states in the QHE, this derivation is also unsatisfactory in that it neglects the two-fold degeneracy that should be associated with spin-1/2 particles. The reason that this is generally a reasonable approximation is that the electron spins will also lead to a Zeeman splitting [20]

$$E \to E \pm \frac{1}{2} g\mu_{\rm B} B\,. \tag{B9}$$

Since we are interested in the strong field and low temperature regime, the energy cost associated with flipping a given spin is typically very large, so we may neglect the spin degeneracy.

Appendix C: Landau Level Wavefunctions in Symmetric Gauge

Although it has been utilitarian to use Landau gauge when approaching the problem of a single particle in a magnetic field, changing to a rotationally symmetric gauge may also provide some insight; in particular, it will be valuable for analyzing the rotationally symmetric Corbino disk geometry of Appendix D. We therefore choose to work in symmetric gauge

$$\mathbf{A} = -\frac{yB}{2}\hat{\mathbf{x}} + \frac{xB}{2}\hat{\mathbf{y}} = -\frac{1}{2}\mathbf{r}\times\mathbf{B}\,. \tag{C1}$$

We may anticipate that angular momentum $L_z = -i\hbar\partial_\phi$ should be a good quantum number; on states of the form $\psi_m(r,\phi) \sim e^{im\phi} f(r)$, the Hamiltonian acts as

$$\begin{aligned}\hat{H}\psi_m &= \frac{1}{2m_e}\big(\hat{p}_r^2 + (\frac{\hbar m}{\hat{r}} + \frac{eB}{2}\hat{r})^2\big)\psi_m \\ &= -\frac{\hbar^2}{2m_e r}\partial_r(r\partial_r)\psi_m \\ &\quad + \Big(\frac{m_e\omega_B^2}{8}\hat{r}^2 + \frac{\hbar m\omega_B}{2} + \frac{\hbar^2 m^2}{2m_e\hat{r}^2}\Big)\psi_m\,.\end{aligned} \tag{C2}$$

Anticipating a wavefunction damped at large radii for the sake of normalizability, we may define without loss of generality $f(r) = g(r)e^{-r^2/4\ell_B^2}$. The time-independent Schrödinger equation then yields

$$\begin{aligned}&g''(r) + \frac{1}{r}\Big(1 - \frac{r^2}{\ell_B^2}\Big)g'(r) - \frac{m^2}{r^2}g(r) \\ &\quad = \Big(\frac{(m+1)m_e\omega_B}{\hbar} - \frac{2m_e E}{\hbar^2}\Big)g(r)\,.\end{aligned} \tag{C3}$$

Assuming a terminating series solution $g(r) = \sum_k c_k r^k$, one finds recurrence relation

$$\big((k+2)^2 - m^2\big)c_{k+2} = \frac{2m_e}{\hbar^2}\big((m+k+1)\frac{\hbar\omega_B}{2} - E\big)c_k\,. \tag{C4}$$

The series must terminate at both sufficiently large and small (possibly negative) k; if k_0 is the first index such that $c_{k_0} \neq 0$, then we must have $k_0 = -2 \pm m$. We then have $c_{k_0}, c_{k_0+2}, \ldots, c_{k_0+2j}$ non-zero for some $j \geq 0$, and $c_{k_0+2j+2} = 0$; for this to be true, we must have

$$\begin{aligned}E &= \frac{\hbar\omega_B}{2}(m + k_0 + 2j + 1) \\ &= \frac{\hbar\omega_B}{2}(m \pm m + 2j + 1)\,,\end{aligned} \tag{C5}$$

which are indeed the previously determined Landau level energies. In particular, the lowest Landau level (LLL) corresponds to taking the negative sign and $j = 0$; in this case, c_{-m-2} is the only non-zero coefficient in our series solution, and we have eigenfunction

$$\psi_{m,LLL} \sim e^{im\phi} r^m e^{-r^2/4\ell_B^2}\,. \tag{C6}$$

Appendix D: QHE from Gauge Invariance

Although it is intuitively clear from the discussion in Section II B that the existence of Hall plateaux can be explained through localization whilst the Fermi energy lies within a 'mobility gap' in the spectrum, it remains unclear why the Hall resistivity at these plateaux takes the observed values $\rho_{xy} = 2\pi\hbar/\nu e^2$, since these values were naively derived with the assumption that *all* states in the filled Landau levels should be involved in charge transport. The apparent robustness of the quantum Hall state to the macroscopic characteristics of the system and the effects of disorder has motivated a formulation of this effect on the general grounds of gauge invariance. We present such an argument, initially due to Laughlin [11] and revised by Halperin [25], which integrates the previous discussion regarding the role of localized states in preserving exact Hall quantization, following the discussion in [4].

Given the observed insensitivity of the QHE to the global geometric features of the sample, we may choose for the purposes of the following argument a 'Corbino disk' geometry, consisting of a two-dimensional conductive annulus encircling a solenoid with magnetic flux Φ, as depicted in Fig. 8. The disk is also subject to a uniform magnetic field B. The vector potential throughout the disk can be taken to be

$$\mathbf{A}(r) = A_\phi(r)\hat{\boldsymbol{\phi}} = \Big(\frac{Br}{2} + \frac{\Phi}{2\pi r}\Big)\hat{\boldsymbol{\phi}}\,. \tag{D1}$$

If impurities are sufficiently small to be neglected for the

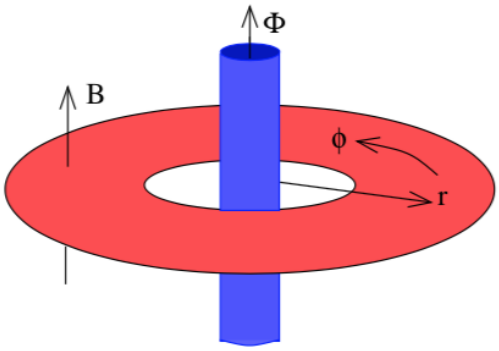

FIG. 8. Corbino disk geometry with magnetic field B, threaded by flux Φ. Figure taken from [4].

time being, the Hamiltonian is then

$$H_\Phi = \frac{1}{2m}\Big[\big(p_r + eA_r\big)^2 + \big(p_\phi + eA_\phi\big)^2\Big] = \frac{1}{2m}\Big[-\frac{\hbar^2}{r}\partial_r\big(r\partial_r\big) + \Big(-i\frac{\hbar}{r}\partial_\phi + \frac{eBr}{2} + \frac{e\Phi}{2\pi r}\Big)^2\Big] \tag{D2}$$

If the flux Φ is taken to vanish, then we simply have the typical QHE Hamiltonian; in this case, the LLL wavefunctions derived in symmetric gauge (see Appendix C) are of the form

$$\psi_m(r,\phi) \sim e^{im\phi} r^m e^{-r^2/4\ell_B^2}\,, \quad m \in \mathbb{Z}\,. \tag{D3}$$

In particular, these wavefunctions are peaked near $r_{\max} \approx \sqrt{2m}\ell_B$. (In fact, our analysis has neglected the fact that the Corbino disk has inner and outer boundaries, so the Hamiltonian should actually have confining potentials at these edges; however, the wavefunctions which are peaked within the available radial range of the disk are suppressed at these boundaries, so we may assume that the Corbino disk supports energy eigenstates which are only slight deformations of the typical LLL states.) If Φ is non-zero, one can verify that the LLL eigenstates are generalized to

$$\psi_m \sim e^{im\phi} r^{m+e\Phi/2\pi\hbar} e^{-r^2/4\ell_B^2}\,. \tag{D4}$$

The naive interpretation is that an increase in the flux Φ should result in outward radial motion of the electron, or charge transport.

We can attempt to 'gauge away' the non-zero flux term from the Hamiltonian, meaning that we can perform a gauge transformation of the form

$$\psi(r,\phi) \to \tilde{\psi}(r,\phi) = e^{-ie\Phi\phi/2\pi\hbar}\psi(r,\phi) \tag{D5}$$

on our wavefunctions, whereupon acting with the Hamiltonian H_Φ on $\tilde{\psi}$ is tantamount to acting with the Hamiltonian $H_{\Phi=0}$ on the state ψ. This simply amounts to choosing a more convenient gauge in which to approach the quantum mechanical problem, wherein an explicit contribution of the flux to the energy spectrum is now absent. For an extended state, whose wavefunction ψ is non-vanishing throughout the disk, one sees that for such a gauge transformation to leave the wavefunction single-valued, one requires $\frac{e\Phi}{2\pi\hbar} \in \mathbb{Z}$; that is, Φ must be an integer multiple of the flux quantum Φ_0. On the other hand, for a localized state, we can choose the position of the branch cut for the phase such that it coincides with a region where the wavefunction vanishes; thus, we have no such quantization criterion in this case. As a result, we see that the energies of localized states are insensitive to the flux Φ, whereas those of the extended states are sensitive to the non-integer part of Φ/Φ_0.

One might expect, therefore, that if the system begins in an energy eigenstate ψ_m, and Φ is increased from zero to Φ_0, then the system will end in the state ψ_m, given that the flux has changed by an integer multiple of Φ_0. However, if the change occurs as an adiabatic (quasistatic) time-dependence in the Hamiltonian, over a time period $T \gg \omega_B^{-1}$, then the states will in fact undergo *spectral flow*; although the spectrum will return to its initial form, the indiviual states ψ_m will be shifted $\psi_m \to \psi_{m+1}$. We can argue heuristically that this should occur on the basis of the above observation that increasing Φ results in outward radial transport. If we have ν Landau levels, the result is that charge $-\nu e$ is transported outward through any concentric ring within the disk in a time T; this is interpreted as a radial current $I_r = -e/T$. The state nearest the outermost edge of the disk can only flow to the edge; we therefore transport one 'edge mode' to the outer edge of the disk for each filled Landau level. The introduction of the flux is also accompanied by an induced EMF in the disk as a result of Faraday's law, with $\mathcal{E}_\phi = -\partial_t\Phi \approx -\Phi_0/T$. We have thus recovered that an EMF in the azimuthal direction results in a current in the radial direction, from which we may infer the typical Hall resistivity

$$\rho_{r\phi} = \frac{\mathcal{E}_\phi}{I_r} = \frac{2\pi\hbar}{\nu e^2}\,. \tag{D6}$$

The key realization is that, since the flux term in the Hamiltonian can always be gauged away for localized states, these states do not undergo spectral flow; in particular, they do not transport charge as the flux Φ is increased. Nonetheless, we have found that, regardless of how many states in each Landau level actually participate in transport, we recover the same values for the Hall plateaux.

Appendix E: Linear Response and the Kubo Formula

One motivation for considering two-point functions in quantum mechanics is that these objects encode

the linear response behaviour of a quantum mechanical system. Consider some unperturbed, multi-particle, Heisenberg-picture Hamiltonian H_0, to which we add a time-dependent source term

$$H_{\text{source}}(t) = \sum_i \phi_i(t)\mathcal{O}_i(t)\,, \tag{E1}$$

where $\mathcal{O}_i(t)$ are Heisenberg picture observables; we will assume that the sources ϕ_i are small, so that we can use perturbation theory. By definition, states in the interaction picture evolve according to

$$i\partial_t|\psi(t)\rangle_I = H_{\text{source}}|\psi(t)\rangle_I\,; \tag{E2}$$

the solution to this first order ODE is the state

$$|\psi(t)\rangle_I = U(t,t_0)|\psi(t_0)\rangle_I\,, \tag{E3}$$

where we have implicitly defined the unitary operator

$$\begin{aligned} U(t,t_0) &= e^{iH_0(t-t_0)}e^{-iH(t-t_0)} \\ &= \mathbb{T}\,\exp\Big(-i\int_{t_0}^{t} H_{\text{source}}(t')dt'\Big)\,, \end{aligned} \tag{E4}$$

with $\mathbb{T}$ denoting time-ordering within the Taylor expansion of the exponential (see e.g. [26] for details). In particular, if the system is initialized in some state $|\Omega\rangle$ in the distant past $t\to-\infty$, then the expectation value for the operator $\mathcal{O}_i$ at later times (in the presence of sources ϕ_j) is

$$\begin{aligned} \langle\mathcal{O}_i\rangle_\phi &= \langle\Omega|U(-\infty,t)\mathcal{O}_i(t)U(t,-\infty)|\Omega\rangle \\ &= \langle\Omega|\Big(\mathcal{O}_i(t) + i\int_{-\infty}^{t} dt'[H_{\text{source}}(t'),\mathcal{O}_i(t)] + \dots\Big)|\Omega\rangle \\ &\approx \langle\mathcal{O}_i\rangle_{\phi=0} + i\int_{-\infty}^{t} dt'\langle[H_{\text{source}}(t'),\mathcal{O}_i(t)]\rangle\,, \end{aligned} \tag{E5}$$

where we have truncated to first order in the sources. We can express this result as

$$\begin{aligned} \delta\langle\mathcal{O}_i\rangle &\equiv \langle\mathcal{O}_i\rangle_\phi - \langle\mathcal{O}_i\rangle_{\phi=0} \\ &= i\sum_j\int_{-\infty}^{t} dt'\,\langle[\mathcal{O}_j(t'),\mathcal{O}_i(t)]\rangle\phi_j(t')\,, \end{aligned} \tag{E6}$$

which is referred to as the *Kubo formula*. This expression encapsulates the system's response to turning on the various sources at the linearized level.

In the quantum Hall case, the field to be turned on is an electric field $\mathbf{E}(t) = \mathbf{E}e^{-i\omega t}$, the source is some current density $\mathbf{J}$, and the response function of interest is the conductivity σ_{ij}. Working in the Weyl gauge $A_t = 0$, the source term is simply the coupling of the current to the gauge potential

$$H_{\text{source}} = -\mathbf{J}\cdot\mathbf{A}\,, \tag{E7}$$

where explicitly, one has

$$\mathbf{A} = \frac{1}{i\omega}\mathbf{E}e^{-i\omega t} \tag{E8}$$

for our AC electric field. Applying the above generalized analysis to the present situation, we find

$$\delta\langle J_i\rangle = \frac{1}{\hbar\omega}\sum_j\int_{-\infty}^{t} dt'\langle[J_j(t'),J_i(t)]\rangle E_j e^{-i\omega t'}\,, \tag{E9}$$

where we have manually restored factors of $\hbar$. If we henceforth fix the state $|\Omega\rangle$ to be an eigenstate $|m\rangle$ of the unperturbed Hamiltonian, with $H_0|m\rangle = E_m|m\rangle$, we have at this level in perturbation theory

$$\begin{aligned} \langle[J_j(t'),J_i(t)]\rangle &= \langle e^{-iE_mt/\hbar}J_j(t')J_i(t)e^{iE_mt/\hbar}\rangle \\ &\quad - \langle e^{-iE_mt/\hbar}J_i(t)J_j(t')e^{iE_mt/\hbar}\rangle \\ &= \langle e^{-iH_0t'/\hbar}J_j(t')J_i(t)e^{iH_0t'/\hbar}\rangle \\ &\quad - \langle e^{-iH_0t'/\hbar}J_i(t)J_j(t')e^{iH_0t'/\hbar}\rangle \\ &= \langle J_j(0)J_i(t-t')\rangle \\ &\quad - \langle J_i(t-t')J_j(0)\rangle \\ &= \langle[J_j(0),J_i(t-t')]\rangle\,; \end{aligned} \tag{E10}$$

that is, the two-point function depends only on the time difference $s = t-t'$. We may therefore rewrite the above as

$$\delta\langle J_i\rangle = \frac{1}{\hbar\omega}\sum_j\int_0^\infty ds\langle[J_j(0),J_i(s)]\rangle E_j e^{-i\omega(t-s)}\,. \tag{E11}$$

Specifically, we have

$$\delta\langle J_i\rangle = \sum_j \sigma_{ij}(\omega)E_j e^{-i\omega t} \tag{E12}$$

implicitly defining the frequency-space response function

$$\sigma_{ij}(\omega) = \frac{1}{\hbar\omega}\int_0^\infty ds\langle[J_j(0),J_i(s)]\rangle e^{i\omega s}\,. \tag{E13}$$

Now, if we insert a complete set of eigenstates for the unperturbed Hamiltonian, then we find

$$\begin{aligned} \sigma_{ij}(\omega) &= \frac{1}{\hbar\omega}\int_0^\infty ds\, e^{i\omega s}\sum_n\Big(\langle m|J_j(0)|n\rangle\langle n|J_i(s)|m\rangle \\ &\qquad - \langle m|J_i(s)|n\rangle\langle n|J_j(0)|m\rangle\Big) \\ &= \frac{1}{\hbar\omega}\sum_{n\neq m}\int_0^\infty ds\, e^{i\omega s} \\ &\qquad \Big(\langle m|J_j|n\rangle\langle n|J_i|m\rangle e^{-i(E_m-E_n)s/\hbar} \\ &\qquad - \langle m|J_i|n\rangle\langle n|J_j|m\rangle e^{-i(E_n-E_m)s/\hbar}\Big) \end{aligned} \tag{E14}$$

where we have defined $J_k \equiv J_k(0)$, and noted that the term with $n = m$ cancels. If we integrate along a slightly deformed contour, or equivalently if we shift the frequency space pole slightly via $\omega \to \omega + i\epsilon$, then we can perform the convergent integrals

$$\int_0^\infty ds e^{i\omega s - \epsilon s} e^{-i(E_m - E_n)s/\hbar} = \Big[\frac{e^{i\omega s - \epsilon s} e^{-i(E_m - E_n)s/\hbar}}{i\omega - \epsilon s - i(E_m - E_n)/\hbar}\Big]_0^\infty \to \frac{-i\hbar}{\hbar\omega + E_n - E_m} \,. \tag{E15}$$

We would now like to take a limit $\omega \to 0$, to find the Hall conductivity for a DC electric field. Given that

$$\frac{1}{\hbar\omega + E_n - E_m} \approx \frac{1}{E_n - E_m} - \frac{\hbar\omega}{(E_n - E_m)^2} + \mathcal{O}(\omega^2) \,, \tag{E16}$$

we see that to lowest finite order in ω,

$$\sigma_{ij}(0) = i\hbar \sum_{n \neq m} \frac{\langle m|J_j|n\rangle\langle n|J_i|m\rangle - \langle m|J_i|n\rangle\langle n|J_j|m\rangle}{(E_n - E_m)^2} \,. \tag{E17}$$

In particular, $\sigma_{xy} \equiv \sigma_{xy}(0)$ is what we refer to as the Hall conductivity in the state $|m\rangle$.

Appendix F: QHE in Graphene

As an inherently 2-dimensional structure, graphene also provides an experimentally realizable quantum Hall system. In [17], high-mobility graphene samples were obtained, using a mechanical exfoliation technique similar to that applied in [27]. Graphene layers were deposited on a degenerately doped Si substrate, with a 300 nm insulating SiO_2 layer. The number of layers in each prepared sample was inferred from both atomic force microscopy (AFM) profiles and chromatic shifts in optical microscopy images, allowing single-layer samples to be isolated. To fabricate the Hall-bar type apparatus, electron beam lithography was used to pattern samples, followed by a Cr/Au thin-film deposition.

While the operating principle behind experimental studies of the QHE in graphene is similar to the case of semiconductor devices, the theoretical description must be modified; in particular, a half-integer quantum Hall effect

$$R_{xy}^{-1} = \frac{g_s e}{\Phi_0}\Big(n + \frac{1}{2}\Big) \tag{F1}$$

emerges, with g_s a factor accounting for both spin and sub-lattice degeneracy. This phenomenon can be understood from a simple tight-binding analysis of the hexagonal graphene structure [28–31], which reveals a relativistic dispersion relation near the two inequivalent corners of the Brillouin zone, known as *Dirac points*; the structure near the Dirac points is expected to dominate the dynamics in the continuum limit. The half-integer effect is then seen to be a result of the electron-hole degeneracy in this model, in the limit that the effective *Semenoff mass* of the charge carriers vanishes.

Appendix G: Resistance Standard

As noted in Section IV, two electrical standard units are required in order to represent or measure all other electric units in SI. It is known that the resistance value of a wired resistor drifts over time [32]. On the other hand, the Josephson effect and the quantum Hall effect together provide an accurate and reproducible means of realizing two such electrical units in terms of non-electrical SI units. It was therefore realized that the world-wide consistency of electrical measurements could be improved by assigning constant values to the von Klitzing constant R_K and the Josephson constant $K_J = 2e/h$. In 1990, aggregating data from all relevant experiments prior to June 1988, R_K was assigned the value

$$R_{K-90} = 25812.807\,\Omega \,.$$

This was essentially a weighted average of measurements performed as in Section IV and values based on the calculation of the fine structure constant in terms of the anomalous magnetic moment of the electron [21]. To ensure reproducibility, *Technical Guidelines for Reliable Measurements of the Quantized Hall Resistance* [33] have been established, ensuring that the used QHE device is working in the correct realm.

While the assigned R_{K-90} remains valid at the time of writing, it will most likely be abrogated at the revision of the International System of Units (SI) [34]. As mentioned in Section IV, this revision will result in redundancy in the definition of the von Klitzing constant.